Two Glutamate Residues, Glu 208α and Glu 197β, Are Crucial for Phosphorylation and Dephosphorylation of the Active-Site Histidine Residue in Succinyl-CoA Synthetase†

Marie E. Fraser,*,‡ Michael A. Joyce,§,|| David G. Ryan,§,⊥ and William T. Wolodko§

Department of Biochemistry, University of Western Ontario, London, Ontario, Canada N6A 5C1 and Department of Biochemistry, University of Alberta, Edmonton, Alberta, Canada T6G 2H7

Received July 20, 2001; Revised Manuscript Received October 12, 2001

ABSTRACT: Succinyl-CoA synthetase catalyzes the reversible reaction succinyl-CoA + NDP + P_i ↔ succinate + CoA + NTP (N denoting adenosine or guanosine). The enzyme consists of two different subunits, designated α and β. During the reaction, a histidine residue of the α-subunit is transiently phosphorylated. This histidine residue interacts with Glu 208α at site I in the structures of phosphorylated and dephosphorylated *Escherichia coli* SCS. We postulated that Glu 197β, a residue in the nucleotide-binding domain, would provide similar stabilization of the histidine residue during the actual phosphorylation/dephosphorylation by nucleotide at site II. In this work, these two glutamate residues have been mutated individually to aspartate or glutamine. Glu 197β has been additionally mutated to alanine. The mutant proteins were tested for their ability to be phosphorylated in the forward or reverse direction. The aspartate mutant proteins can be phosphorylated in either direction, while the E208αQ mutant protein can only be phosphorylated by NTP, and the E197βQ mutant protein can only be phosphorylated by succinyl-CoA and P_i. These results demonstrate that the length of the side chain at these positions is not critical, but that the charge is. Most significantly, the E197βA mutant protein could not be phosphorylated in either direction. Its crystal structure shows large differences from the wild-type enzyme in the conformation of two residues of the α-subunit, Cys 123α−Pro 124α. We postulate that in this conformation, the protein cannot productively bind succinyl-CoA for phosphorylation via succinyl-CoA and P_i.

The reversible reaction catalyzed by succinyl-CoA synthetase (SCS)[1] is thought to occur via three partial reactions:

$$E + \text{succinyl}-CoA + P_i \leftrightarrow E\cdot\text{succinyl-}PO_3 + CoA \quad (1)$$

$$E\cdot\text{succinyl}-PO_3 \leftrightarrow \text{succinate} + E-PO_3 \quad (2)$$

$$E-PO_3 + NDP \leftrightarrow NTP + E \quad (3)$$

where E denotes the enzyme, E·succinyl-PO_3 designates the noncovalent association of SCS with succinyl phosphate, and N denotes adenosine or guanosine (*1*, *2*). SCS consists of two different subunits, designated α and β. In the reaction, the enzyme is phosphoryated on the Nε2 atom of an essential histidine residue of the α-subunit, either by succinyl phosphate or by nucleotide triphosphate.

The first structure determination of SCS showed that the phosphorylated histidine residue, His 246α[2] in *Escherichia coli* SCS, interacts with residues from each of the subunit types (*3*). The phosphoryl group is positioned at the amino-termini of two α-helices named the "power" helices, one of

† This work was funded by research grants from the Natural Sciences and Engineering Research Council of Canada (NSERC) and the Canadian Institutes of Health Research. M.E.F. is supported by an NSERC University Faculty Award. Crystallization and computational resources were purchased with awards from the Academic Development Fund, University of Western Ontario (project 00-152) and the Canada Foundation for Innovation (project 3185). The crystallographic data were collected at two synchrotron sources: the Cornell High Energy Synchrotron Source (CHESS) and the Stanford Synchrotron Radiation Laboratory (SSRL). Research conducted at CHESS is supported by the National Science Foundation under award DMR-9311772, using the Macromolecular Diffraction at CHESS (MacCHESS) facility, which is supported by award RR-01646 from the National Institutes of Health. SSRL is a national user facility operated by Stanford University on behalf of the U.S. Department of Energy, Office of Basic Energy Sciences. The SSRL Structural Molecular Biology Program is supported by the Department of Energy, Office of Biological and Environmental Research, and by the National Institutes of Health, National Center for Research Resources, Biomedical Technology Program funded by the Department of Energy (BES, BER) and the National Institutes of Health (NCRR, NIGMS).

* To whom correspondence should be addressed. Phone: (519) 661-3060. Fax: (519) 661-3175. E-mail: mfraser4@uwo.ca.

‡ University of Western Ontario.

§ University of Alberta.

|| Current address: Department of Medical Microbiology and Immunology, University of Alberta, Edmonton, Alberta, Canada T6G 2H7.

⊥ Current address: Department of Dermatology, 415 Curie Boulevard, 230 Clinical Research Building, University of Pennsylvania, Philadelphia, PA 19104.

[1] Abbreviations: SCS, succinyl-CoA synthetase; NDP, adenosine or guanosine 5′-diphosphate; NTP, adenosine or guanosine 5′-triphosphate; DD-ligase, D-Ala:D-Ala ligase; P_i, inorganic phosphate; CoA, coenzyme A; CHESS, Cornell High Energy Synchrotron Source; SSRL, Stanford Synchrotron Radiation Laboratory; F_o, observed structure factor amplitude; F_c, structure factor amplitude calculated from the model; α_c, phase calculated from the model; σ, standard deviation.

[2] Specific amino acid residues in SCS are designated by the one- or three-letter code followed by the residue number and either α or β to indicate the subunit. The mutations are indicated using one letter code, X#(subunit)Y, where X is the residue type in the wild-type enzyme, # is the residue number, (subunit) is α or β and Y is the residue type in the mutant.

10.1021/bi011518y CCC: $22.00
Published on Web 12/14/2001

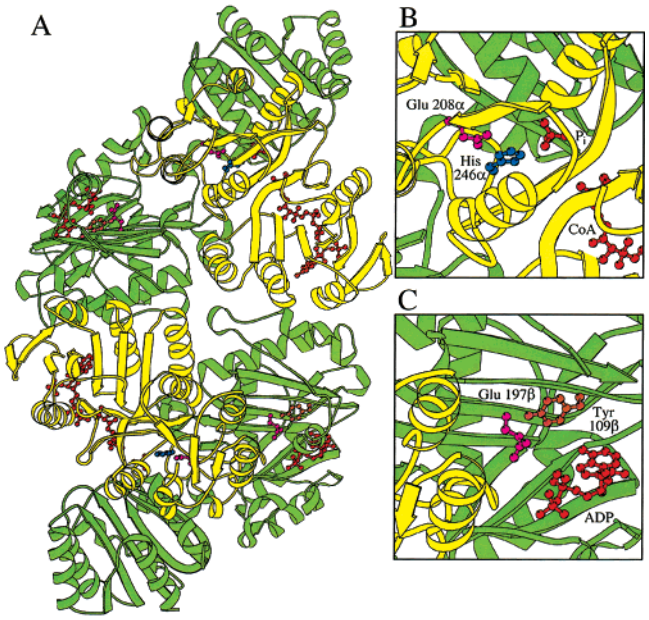

FIGURE 1: (A) Ribbon diagram of the $\alpha_2\beta_2$-heterotetramer of *E. coli* succinyl-CoA synthetase in complex with Mg^{2+}-ADP [PDB coordinates 1CQJ (*4*)]. The panels on the right show close-up views of (B) Glu 208α and (C) Glu 197*β* and their environments. The side chains of these glutamate residues, as well as the side chains of His 246α and Tyr 109*β*, and the substrates CoA, P_i and ADP are shown as ball-and-stick models. The two glutamate residues are colored in magenta, His 246α in blue, Tyr 109*β* in brown and the substrates in red. The ribbons representing the α-subunits are yellow, and those representing the *β*-subunits are green. Parts of the ribbon diagram that would occlude the catalytic residues or the substrates have been removed from the close-up views, but the orientation of the heterotetramer is identical in all three diagrams. Note that panel B focuses on site I of the α*β*-dimer shown at the top in panel A, while panel C focuses on site II of the α*β*-dimer shown at the bottom. This figure and Figure 6 were drawn using the program MOLSCRIPT (*40*).

which is contributed by the α-subunit and the second by the *β*-subunit. The imidazole ring of His 246α interacts with the side chain of a glutamate residue of the α-subunit, Glu 208α. The carboxylate group of Glu 208α accepts a hydrogen bond from Nδ1 of the imidazole ring. The glutamate residue also stabilizes the proton on Nδ1 when His 246α is not phosphorylated, yet binds a phosphate ion at the same site (Figure 1A and B) (*4*, *5*). A molecule of CoA is bound to the α-subunit with its free thiol group located 3.5 Å from the nearest oxygen atom of the phosphohistidine residue (*3*, *6*). This site where CoA and, presumably, succinate bind has been designated site I (*7*).

In the structure of *E. coli* SCS in complex with Mg^{2+}-ADP, the ligand Mg^{2+}-ADP is bound in the *β*-subunit approximately 35 Å from the active-site histidine residue (*4*). This nucleotide-binding site had been predicted (*6*) based on the structure of D-Ala:D-Ala ligase (DD-ligase) (*8*). Like SCS, DD-ligase possesses what has been named the "ATP-grasp fold" (*9*). When the structure of DD-ligase was determined, this fold had been observed in only two structures, glutathione synthetase (*10*) and SCS. The structure of DD-ligase was determined in complex with ADP, Mg^{2+} ions, and a phosphorylated phosphinate analogue of the substrate, revealing the role of this new fold. Since then, a number of other proteins have been shown to possess the ATP-grasp fold, including biotin carboxylase (*11*), pyruvate phosphate dikinase (*12*), an ATP-dependent DNA ligase (*13*), an mRNA capping enzyme (*14*), carbamoyl phosphate synthetase (*15*), synapsin I (*16*), glycinamide ribonucleotide synthetase (*17*) and *N*5-carboxyaminoimidazole ribonucleotide synthetase (*18*). All are known to bind nucleotide, and many of the amino acid residues important in the nucleotide binding are "conserved" among these proteins. Although the enzymes have a common fold for binding the nucleotide, they have different binding sites for the substrate that is phosphorylated in the reaction. In SCS, this substrate is the active-site histidine residue. However, the nucleotide-binding site, which we refer to as site II (*7*), is located far from where the active-site histidine residue is observed in our structures (Figure 1A) (*3*−*6*). It was thus postulated that the loop containing the active-site histidine residue swings to shuttle the phosphoryl group between site I, the binding-site for CoA and succinate, and site II, where the nucleotide binds (*4*, *6*).

We hypothesized that a second glutamate residue, or a residue with similar functionality, must interact with Nδ1 of the active-site histidine residue during phosphorylation or dephosphorylation by nucleotide at site II (*6*). In the structure of the complex with DD-ligase, the phosphorylphosphinate inhibitor interacts with Arg 255, a residue that donates two hydrogen bonds to the two oxygen atoms of the phosphinate (*8*). In the superposition of the residues of *E. coli* SCS on the residues of DD-ligase that adopt the ATP-grasp fold, Glu 197*β* of SCS superposes with Arg 255. We suggested that Glu 197*β* accepts a hydrogen bond from Nδ1 of His 246α when this active-site residue is swung "down" to site II. The hydrogen-bonding interaction would be analogous to that between Glu 208α and His 246α when His 246α is "up" in site I. The location of Glu 197*β* is shown in Figure 1A and C.

To test this hypothesis and to assess the roles of Glu 197*β* and Glu 208α, each of these residues was mutated. They were individually changed to aspartate residues to shorten the side chain by one methylene group, or to glutamine residues to eliminate the charge on the side chain without changing either its length or its ability to form hydrogen-bonding interactions. Glu 197*β* was mutated additionally to alanine, a more drastic change that would eliminate its ability to interact with the active-site histidine residue. The role of each glutamate residue was evaluated by determining the mutants' abilities to catalyze the partial phosphorylation reactions involving either succinyl-CoA and P_i (partial reactions 1 and 2) or nucleotide (partial reaction 3 in reverse) and by measuring the kinetic parameters of the mutant proteins where possible. We hypothesized that the mutations at site I would affect phosphorylation via succinyl-CoA and P_i but would not affect phosphorylation via nucleotide, whereas mutations at site II would affect phosphorylation via nucleotide but not via succinyl-CoA and P_i. A surprising result occurred with the mutation of Glu 197*β* to alanine. As predicted, this mutation at site II led to a protein that could not be phosphorylated by nucleotide. However, it could not be phosphorylated by succinyl-CoA and P_i either. To investigate how this mutation at site II could affect the partial reactions taking place at site I, the structure of the E197*β*A mutant protein was determined using X-ray crystallography.

MATERIALS AND METHODS

Construction, Expression, and Purification of Site-Directed Mutants. The five mutants were made using standard

protocols for the PCR and overlap extension (*19*). The template for PCR was the plasmid pGS202 (*20*), and the primers for the construction of the mutant plasmids were as follows: for mutations of Glu 208α, the 5′-flanking primer 5′-GCCCGCTATGGCTTACCAGC-3′, the 3′-flanking primer 5′-GGTCGACGAATTCCGGACA-3′ (in the multiple cloning site of pGS202 downstream of the α-subunit), and the internal primers 5′-CGTGATGATCGGT**GAT**ATCGGCG-GTAGCG-3′ and its complement for the mutation to Asp and 5′-CGTGATGATTGGC**CAG**ATCGGCGGTA-3′ and its complement for the mutation to Gln; for mutations of Glu 197*β*, the 5′-flanking primer 5′-GCCCGCTATGGCT-TACCAGC-3′, the 3′-flanking primer 5′-CCTCCACTGCG-GCAACAACC-3′, and the internal mutagenic primers 5′-GGCGTTGATC**CAA**ATCAACC-3′ and its complement for the mutation to Gln and the mixture of primers 5′-GCGT-TGATC(**A**/**G**/**C**)(**A**/**C**)(**G**/**C**)ATCAACCCG-3′ and complements for the mutations to Asp and Ala. The nucleotides shown in bold are the ones that lead to the mutation. The entire gene fragment created by PCR mutagenesis and the flanking regions were sequenced to verify the constructs. The mutant fusion product for the mutation E208αD or E208αQ and the vector pGS202 was digested with *Avr*II and *Eco*RI. The mutant fusion product for the mutation E197*β*Q, E197*β*D, or E197*β*A and the vector pGS202 was digested with *Bst*XI and *Bpu*1102I. The presence of each mutation was verified by DNA sequencing using an Applied Biosystems model 373 automated sequencer.

The SCS null strain TK3D18 (*21*) was transformed with the mutant plasmids. Mutant proteins were expressed and purified in high yields (approximately 30−100 mg/L of culture) using the methods previously described (*3*, *22*). The gel filtration step of the purification scheme demonstrated that each of the mutant proteins was a heterotetramer, just like wild-type SCS. The mutant proteins were stored at 4 °C as precipitate suspensions by adding 50 g of $(NH_4)_2SO_4$/100 mL of protein solution.

Phosphorylation Reactions Catalyzed by SCS Mutants. Cell lysates were used to test the ability of each mutant to be phosphorylated. By using cell lysates instead of purified protein, any changes to the mutant protein that might occur during purification were precluded. Any possible biases due to using lysates rather than purified protein were controlled for by synchronizing protein expression from the cells containing the mutant or the wild-type constructs and normalizing the amount of overexpressed protein based on the amounts of the *β*-subunits. The amount of protein used for the phosphorylation was quantified using SDS−PAGE, by staining the protein bands with Coomassie blue and by analyzing the expression of the *β*-subunit of SCS using a Bio-Rad Gel Doc 1000 and the accompanying software. Phosphorylation of SCS using ATP or GTP (partial reaction 3) was carried out at 22 °C in 30 μL of a buffer containing 10 mM $MgCl_2$, 50 mM KCl, and 50 mM Tris-HCL (pH 7.4) with 1 mM [γ-^{32}P]ATP or [γ-^{32}P]GTP (approximately 0.3 C_i/mmol). The reaction was started by the addition of 5 μg in 2 μL of lysate, and the mixtures were incubated for various lengths of time before the addition of 15 μL of SDS−PAGE loading buffer to stop the reaction. Phosphorylation in the opposite direction via succinyl-CoA and P_i (partial reactions 1 and 2) was carried out in the same buffer except that [γ-^{32}P]-ATP or [γ-^{32}P]GTP was replaced by 0.3 mM succinyl-CoA and 1 mM $^{32}P_i$ (approximately 0.3 C_i/mmol). The results were analyzed via SDS−PAGE [12% (w/v) polyacrylamide gels] and autoradiography, with the radioactively labeled bands quantified by phosphorimaging. Exposure of the image plate was complete in 1−2 h. Note that although the radioactively labeled bands were quantified, these initial experiments were designed solely to test whether the α-subunit could be phosphorylated by each partial reaction.

Steady-State Kinetic Analyses of SCS Mutants. For kinetic analyses, an aliquot of the purified protein in $(NH_4)_2SO_4$ suspension was centrifuged (15000*g* for 30 min at 4 °C) and the pellet was dissolved in 500 μL of 50 mM KCl, 0.1 mM EDTA, and 50 mM Tris-HCl (pH 7.4). The solution was clarified of particulate matter and denatured protein by centrifugation (15000*g* for 30 min at 4 °C) and dialyzed at 4 °C for 16 h with three changes of the same buffer. The concentration of the protein was determined spectrophotometrically using the extinction coefficient determined for wild-type SCS at 280 nm ($E^{1\%}_{1cm} = 5.0$) (*23*). The concentrations of the nucleotides and CoA were determined using their standard extinction coefficients for a 1 cm path length: for ATP, $E_{259nm} = 15.4\ mM^{-1}$, for GTP, $E_{252nm} = 13.7\ mM^{-1}$, and for CoA, $E_{260nm} = 14.6\ mM^{-1}$. For each substrate, the initial velocity was measured at various concentrations with a constant concentration of the other substrates (129 μM CoA, 10 mM succinate and 441 μM ATP, as appropriate) in a 1 mL volume of 50 mM KCl, 10 mM $MgCl_2$ and 50 mM Tris-HCl (pH 7.4). Initial rates were measured in duplicate at 22 °C and the data were analyzed using the ENZYME KINETICS 1.11 program for Macintosh computers (*24*).

Crystallographic Analysis of the Wild-Type Enzyme and of the E197βA Mutant Protein. All of the steps to prepare the protein samples for crystallization were performed at 4 °C. The protein from aliquots of the ammonium sulfate suspension of purified wild-type enzyme or of the purified E197*β*A mutant protein was collected by centrifugation, dissolved in 50 mM potassium phosphate (pH 7.4), and dialyzed against the same buffer to remove residual ammonium ions. Still in their respective dialysis bags, these protein solutions were transferred to a solution consisting of 5 mM ATP and 50 mM $MgCl_2$ in 50 mM MOPS (pH 7.4) or in 50 mM Bicine (pH 7.6) for 12 h for possible phosphorylation. To remove any nucleotide, these solutions were dialyzed extensively against several changes of buffer: 50 mM potassium phosphate (pH 7.4) for the wild-type enzyme, and 50 mM potassium phosphate (pH 7.4) followed by 50 mM Bicine (pH 7.6) for the E197*β*A mutant protein. Crystals of the wild-type enzyme in complex with CoA were grown by microdialysis as previously described (*25*). Crystals of the E197*β*A mutant protein in complex with CoA were grown by vapor diffusion in hanging drops. In the vapor diffusion experiments, the reservoir solutions consisted of 1 mL of 100 mM Bicine (pH 7.6) and 1.80−2.04 M $(NH_4)_2SO_4$. The drop was formed from 2 μL volumes of the reservoir solution and the protein stock solution (13.8 mg/mL protein, 0.5 mM CoA). Crystals appeared in 3−4 months at 21 °C.

To collect the diffraction data, crystals were cryoprotected by gradually increasing the concentration of glycerol in the mother liquor to 25% (v/v). They were then vitrified in a

cold nitrogen stream at 100 K. The data from the wild-type enzyme were collected on the CHESS A-1 beamline with a wavelength of 0.935 Å, using the Quantum-4 Area Detector Systems CCD (*26*). Crystals of the E197βA mutant protein were stored in liquid nitrogen and shipped for data collection on beamline 9-1 at SSRL using X-rays with a wavelength of 0.979 Å and a MAR345 image plate detector (X-ray Research BmbH). The two data sets were processed using the HKL processing package (*27*).

The starting model for the refinement was the previously published structure of *E. coli* succinyl-CoA synthetase (*6*). This coordinate set was refined initially using the cryodata from the wild-type enzyme, and the subsequent partially refined model was also refined using the data from the crystal of the E197βA mutant protein. Both refinements used the maximum likelihood target in CNS (*28*), iterative steps of refinement and rebuilding of the model with the program TOM (*29*), and checks of the stereochemistry of the models using the programs PROCHECK (*30*) and WHATCHECK (*31*). The CCP4 Suite provided the framework for the crystallographic calculations, including analysis of the models (*32*).

RESULTS

Partial reaction experiments were performed with succinyl-CoA and $^{32}P_i$ (partial reactions 1 and 2) or [γ-^{32}P]ATP or [γ-^{32}P]GTP (partial reaction 3) to determine if any of the partial reactions were impaired by the mutations of Glu 208α or Glu 197β. As can be seen in Figure 2A, the α-subunit of the E208αQ mutant protein was not phosphorylated by succinyl-CoA and $^{32}P_i$, but the E208αD mutant protein was, in a manner similar to wild-type SCS. Both of these mutants were phosphorylated by [γ-^{32}P]ATP or by [γ-^{32}P]GTP, as was wild-type SCS (Figure 2B and C). In contrast, the E197βQ mutant protein was not phosphorylated by [γ-^{32}P]-ATP nor by [γ-^{32}P]GTP (Figure 3B and C). The E197βD mutant protein was phosphorylated by [γ-^{32}P]ATP or by [γ-^{32}P]GTP, in a manner similar to wild-type SCS (Figure 3B and C). Both the E197βD and the E197βQ mutant proteins were phosphorylated like the wild-type SCS via succinyl-CoA and $^{32}P_i$ (Figure 3A). The E197βA mutant protein was not phosphorylated by either succinyl-CoA and $^{32}P_i$ or radioactively labeled nucleotide (Figure 3A, B, and C).

The kinetic parameters were measured for four of the mutant proteins, omitting the E197βA mutant because of its very low activity. The values of $K_{m(app)}$ for succinate, CoA, ATP, and GTP, as well as the values of k_{cat}, using ATP or GTP, were determined from the kinetic analyses and are presented in Table 1. For both the E208αD and the E208αQ mutant proteins, the values of $K_{m(app)}$ for succinate, CoA and ATP were comparable to those observed with wild-type SCS. However, while the $K_{m(app)}$ value for GTP with the E208αD mutant protein was comparable to that observed with wild-type SCS, the value with the E208αQ mutant protein was 36 times lower than that with the wild-type enzyme. While the two values of k_{cat} for the E208αD mutant protein were comparable to those for wild-type SCS, the two values of k_{cat} for the E208αQ mutant protein were reduced approximately 5000-fold. The $K_{m(app)}$ and k_{cat} values with the E197βD mutant protein were comparable to those of wild-type SCS. The $K_{m(app)}$ value for each substrate with the E197βQ mutant protein was comparable to that with the wild-type enzyme, except for GTP, whose $K_{m(app)}$ value was reduced by a factor of 20. Similar to the results for the E208αQ mutant protein, the k_{cat} value with the E197βQ mutant had decreased 3000-fold from the wild-type SCS when using ATP and 7000-fold when using GTP.

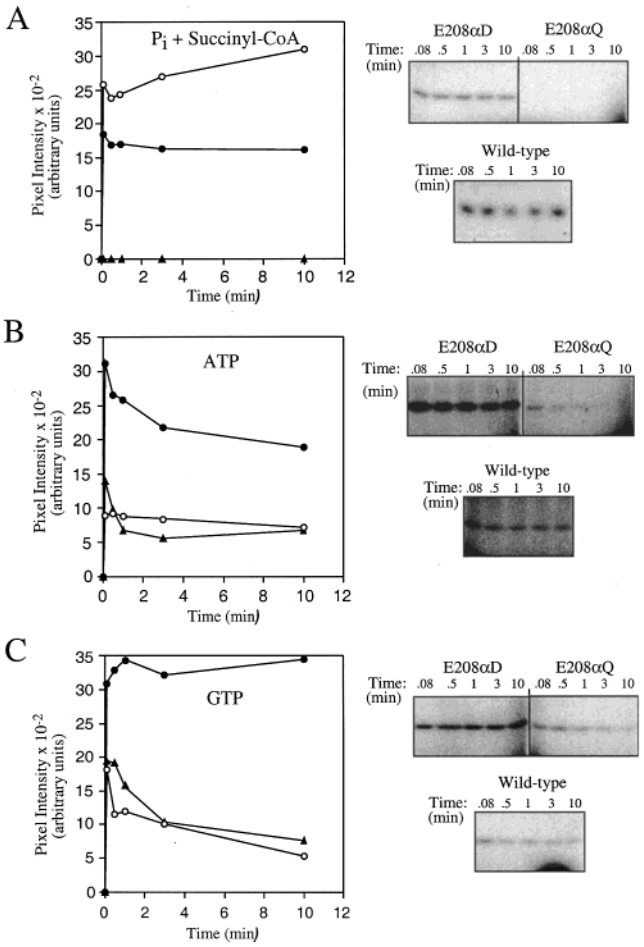

FIGURE 2: Time course for the phosphorylation of wild-type SCS and of the E208αD and E208αQ mutant proteins. The proteins were incubated in the presence of (A) succinyl-CoA and $^{32}P_i$, (B) [γ-^{32}P]-ATP, or (C) [γ-^{32}P]GTP. Samples were taken at the times listed and analyzed by SDS−PAGE. (See Materials and Methods for full experimental details.) Autoradiographs on the right show phosphorylation of the α-subunit. The results were quantified using phosphorimagery and are plotted on the left: (○) wild-type SCS, (●) E208αD mutant protein, and (▲) E208αQ mutant protein.

The E197βA mutant protein crystallized in the same space group as wild-type SCS. However, the crystals grew as plates rather than as the cubes which are the usual crystal habit for wild-type SCS. X-ray crystallographic data were collected at low temperature (100 K) to reduce decay. This allowed a complete data set to be collected from a single crystal of each protein. Pertinent statistics about the data sets are included in Table 2.

The first cycles of refinement of the model for wild-type SCS accommodated the changes in the unit cell dimensions of the cryoprotected crystal at low temperature. The $2F_o - F_c$, α_c electron density map for wild-type SCS showed clear electron density for the side chain of Glu 197β. Initial $F_o - F_c$, α_c electron density maps for the E197βA mutant protein had negative density at the site of the mutation. This

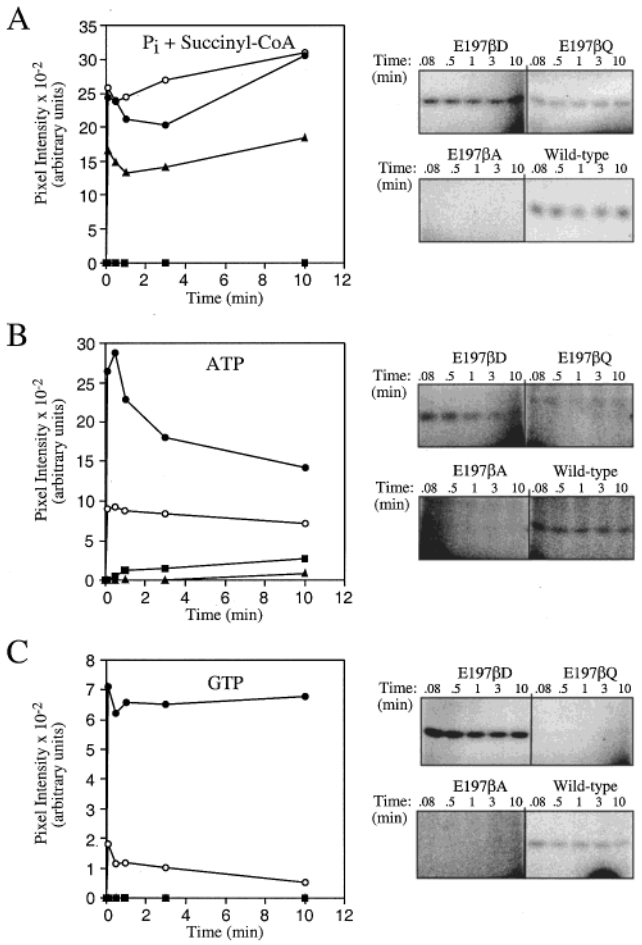

FIGURE 3: Time course for the phosphorylation of wild-type SCS and of the E197βD, E197βQ, and E197βA mutant proteins. The proteins were incubated in the presence of (A) succinyl-CoA and $^{32}P_i$, (B) [γ-^{32}P]ATP, or (C) [γ-^{32}P]GTP. Samples were taken at the times listed and analyzed by SDS−PAGE. (See Materials and Methods for full experimental details.) Autoradiographs on the right show phosphorylation of the α-subunit. The results were quantified using phosphorimagery and are plotted on the left: (○) wild-type SCS, (●) E197βD mutant protein, (▲) E197βQ mutant protein, and (■) E197βA mutant protein.

disappeared when the side chain of the residue in the model was truncated to Cβ. There was also negative electron density and residual positive electron density in the $F_o - F_c$, α_c maps and poor fit of the model to the $2F_o - F_c$, α_c electron density near residues 123 and 124 of the α-subunit (Figure 4A). The model was refitted in this region: the side chain of Pro 124α was flipped to the interior of the protein to occupy the position of the side chain of Cys 123α in the previous model and the side chain of the cysteine residue was flipped to the exterior of the protein (Figure 4B). There was no electron density for the free thiol end of the CoA molecule, so the last six atoms [PC5(═PO5)−PN4−PC3−PC2−PS1] were removed from the model.

Table 2: Statistics for the Two Crystallographic Data Sets, Wild-Type *E. coli* SCS and the E197βA Mutant Protein

data set	wild-type SCS	E197βA mutant
resolution range for data processing (Å)	20−2.4	100−2.7
no. of measurements	156 588	152 728
no. of unique reflections	68244	48720
R_{merge}[a](%)	5.3	4.1
R_{merge} in high-resolution shell (%)	32.4	33.8
(resolution range)	(2.44−2.4)	(2.75−2.7)
$\langle I\rangle/\langle\sigma(I)\rangle$[a]	14	28
$\langle I\rangle/\langle\sigma(I)\rangle$ in high-resolution shell	2.5	2.6
(resolution range)	(2.44−2.4)	(2.75−2.7)
completeness (%)	89.4	91.0
completeness in high-resolution shell (%)	73.5	61.7
(resolution range)	(2.44−2.4)	(2.75−2.7)

[a] $R_{merge} = (\Sigma\Sigma|I_i - \langle I\rangle|)/\Sigma\Sigma\langle I\rangle$, where I_i is the intensity of an individual measurement of a reflection and $\langle I\rangle$ is the mean value for all equivalent measurements of this reflection. [b] $\langle I\rangle$ is the mean intensity for all reflections, $\langle\sigma(I)\rangle$ is the mean sigma for these reflections.

The results of the two refinements are summarized in Table 3. The refined coordinate sets, as well as the structure factors, have been submitted to the Protein Data Bank (*33*) where they are identified by the codes 1JKJ for the wild-type enzyme and 1JLL for the E197βA mutant protein.

DISCUSSION

The two glutamate residues, Glu 208α and Glu 197β, were mutated to test their roles in the catalytic mechanism of SCS. Glu 208α is located at site I of the enzyme, where the partial reactions 1 and 2 leading to phosphorylation of the enzyme by succinyl-CoA and phosphate take place (*3*). Glu 197β is located at site II where the nucleotide binds and partial reaction 3 occurs (*4*, *6*). By attempting to phosphorylate the mutant proteins via the appropriate partial reactions, we could judge whether these glutamate residues were important in catalyzing the phosphorylation steps at site I or II. The mutation of Glu 208α to a glutamine residue impaired phosphorylation by succinyl-CoA and P_i. This result was expected, since this glutamate residue had been seen in the crystal structures to interact with the active-site histidine residue at site I where CoA and phosphate bind. The glutamate residue accepts a hydrogen bond from atom Nδ1 of the imidazole ring, ensuring that atom Nϵ2 is unprotonated, with the lone pair electrons available for nucleophilic attack on the phosphoryl group of succinyl-phosphate. The

Table 1: Kinetic Parameters of Wild-Type and Mutant SCS Proteins[a]

protein	succinate $K_{m(app)}$ (mM)	CoA $K_{m(app)}$ (μM)	ATP $K_{m(app)}$ (μM)	ATP k_{cat} (min^{-1})	GTP $K_{m(app)}$ (μM)	GTP k_{cat} (min^{-1})
wild-type[b]	0.25	4.0 ± 0.8	70 ± 18	2684	394 ± 55	1471
mutations of Glu 208α (site I)						
E208αD	0.26 ± 0.04	2.0 ± 0.3	116 ± 20	2343	63 ± 19	539.6
E208αQ	0.27 ± 0.02	1.3 ± 0.1	41 ± 8	0.57	11 ± 3	0.28
mutations of Glu 197β (site II)						
E197βD	0.87 ± 0.03	2.7 ± 0.7	137 ± 27	1775	311 ± 50	1775
E197βQ	0.4 ± 0.1	1.8 ± 0.3	106 ± 9	0.85	20 ± 3	0.21

[a] Measured by following the production of succinyl-CoA spectrophotometrically at 235 nm. See Materials and Methods for specific details. [b] Joyce et al. (*7*).

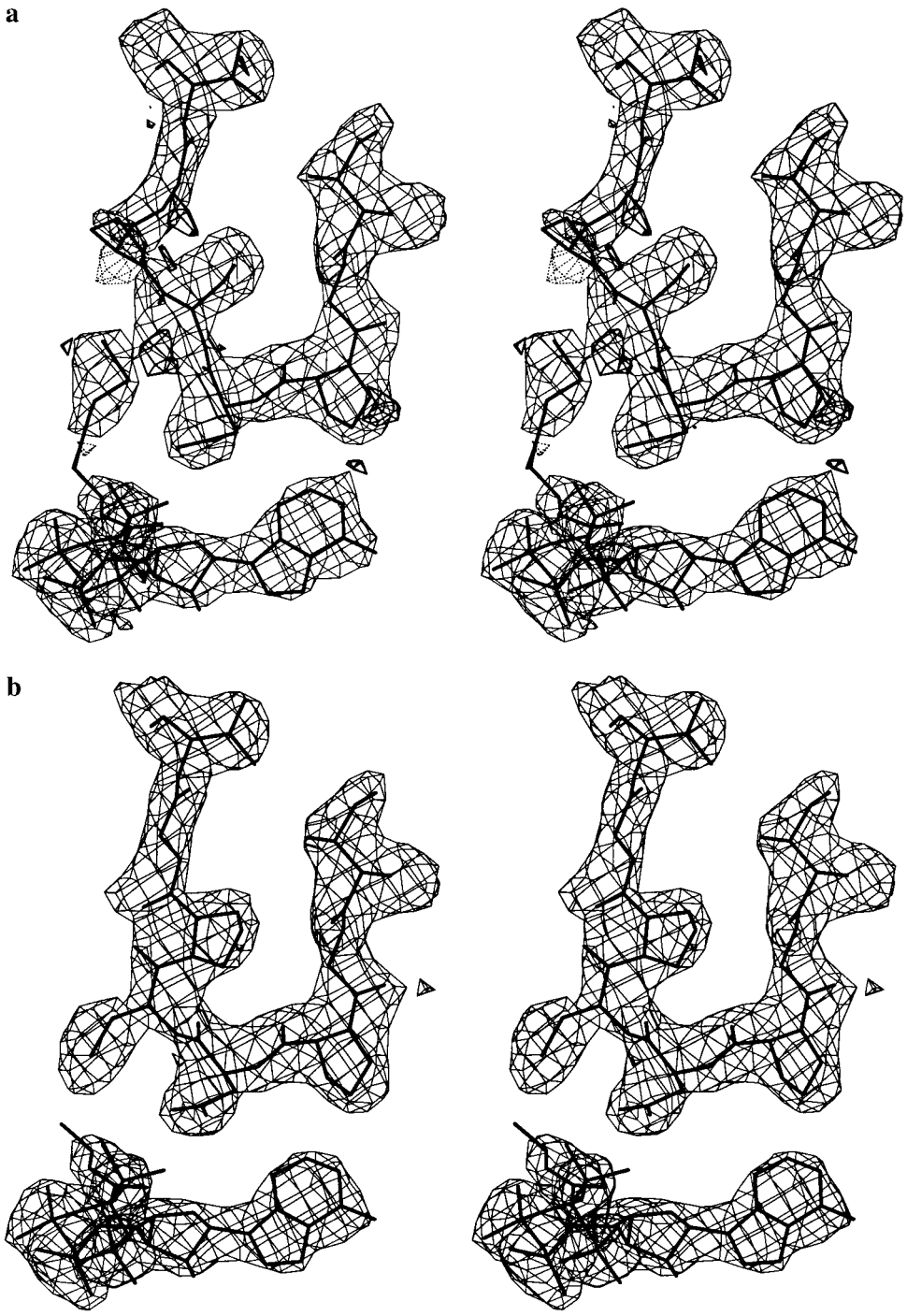

FIGURE 4: Electron density near residues Cys 123α and Pro 124α for the E197βA mutant protein. Part of the model used to calculate the phases is shown as thick lines in this stereo diagram. At the top of the two panels are residues 119−126 of the α-subunit and at the bottom is the molecule of CoA. (A) The $2F_o - F_c$, α_c map contoured at the $+1.5\sigma$ level is drawn with a fine solid line. The $F_o - F_c$, α_c map is contoured at -3σ and $+3\sigma$ and drawn with a dotted line for the negative density (note the negative density near Pro 124α) and a solid line, thicker than that used for the $2F_o - F_c$, α_c map (note the density between the thiol of CoA and Cys 123α and near Pro 121α. The model and maps are those after two cycles of refinement when the residues Cys 123α and Pro 124α were in a similar conformation to that seen in the structure of wild-type SCS. (B) The $2F_o - F_c$, α_c map of the final model after rebuilding and refinement. The electron density map is contoured at the 1.5σ level. Note that the model of CoA is incomplete.

equivalent change of Glu 197β to a glutamine residue impaired phosphorylation by ATP or by GTP. This result supports our hypothesis that Glu 197β serves a similar role to Glu 208α, accepting a hydrogen bond from His 246α when this residue is in position to be phosphorylated by nucleotide at site II.

In contrast to the change of either glutamate residue to glutamine, the change to aspartate had little effect on phosphorylation or on the kinetic parameters of SCS. These results suggest that the charge of the residue at this position is critical, since shortening the side chain by one methylene group did not reduce the enzymatic activity. The distance from atom Nδ1 of His 246α to atom Oε2 of Glu 208α is 2.6 Å in the structure of wild-type SCS, indicating a strong hydrogen bond. We can conclude that the aspartate side chain would still be long enough to form a productive interaction

Table 3: Refinement Statistics for the Two Models, Wild-Type *E. coli* SCS and the E197βA Mutant Protein

	wild-type SCS	E197βA mutant
cell dimensions		
a, *b* (Å)	96.63	97.06
c (Å)	386.8	389.6
α, β, γ (deg)	90	90
resolution range for refinement (Å)	19.64−2.35	34.38−2.69
no. of data	68 151	48 023
completeness (%)	87.7	90.5
R-factor[a] (number of data) (%)	19.2 (67088)	22.2 (47023)
R_{free}[a] (number of data) (%)	23.8 (1063)	25.9 (1000)
no. of protein atoms	9934	9923
no. of water molecules	593	193
no. of ligand atoms	168 (2 molecules CoA, 2 phosphate ions, 4 sulfate ions, 1 molecule glycerol, 2 partial molecules CoA)	139 (2 molecules CoA, 2 phosphate ions, 4 sulfate ions, 2 partial molecules CoA)
rms deviations from ideal geometry		
bond lengths (Å)	0.016	0.017
bond angles (deg)	1.9	2.0
Ramachandran plot statistics for non-proline and non-glycine residues		
no. in most favored regions (%)	1036 (93.0)	978 (87.9)
no. in additional allowed regions (%)	76 (6.8)	134 (11.7)
no. in generously allowed regions (%)	0 (0)	0 (0)
no. in disallowed regions (%)	2 (0.2)	2 (0.2)

[a] $R = \sum ||F_o| - |F_c||/\sum |F_o|$. [b] *R*-factor based on data excluded from the refinement (originally 10%, reduced to approximately 1000 reflections).

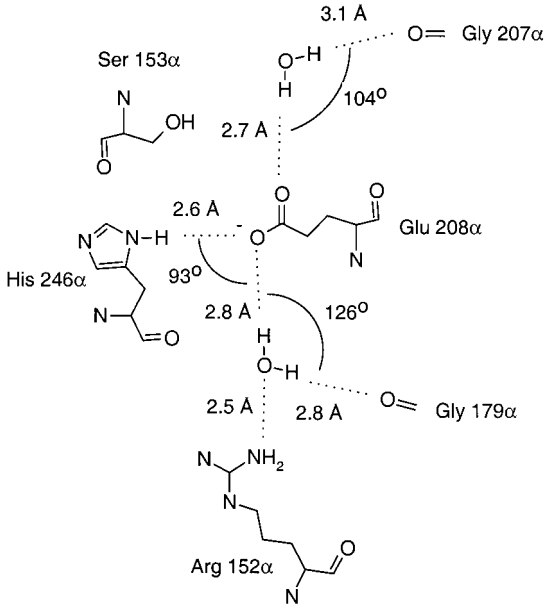

FIGURE 5: Schematic of the likely hydrogen-bonding network at Glu 208α.

with the histidine residue, stabilizing the proton and the positive charge on Nδ1.

The replacement of a glutamate residue by glutamine changes the hydrogen-bonding capability of this residue as well as its charge. Our results suggest that the charge is critical, but the two protons introduced by substituting the amide side chain for the carboxylate may also play a role in reducing catalytic efficiency. Figure 5 depicts the most likely hydrogen-bonding network around Glu 208α in the wild-type enzyme, based on the positions of the atoms in the crystal structure. Ser 153α is included in the diagram because the Cβ atom of Ser 153α is only 3.5 Å from atom Oε1 of Glu 208α. Although Ser 153α does not form a hydrogen bond with Glu 208α since the Oγ atom is directed away from Glu 208α, rotation of the side chain torsion angle could move Oγ into position to accept a hydrogen bond from a glutamine residue in position 208α. Since this serine residue interacts with the phosphate ion at site I of the enzyme (*4*, *5*), any change in its conformation could also affect catalysis. This is only one possibility, but it demonstrates the need to be wary of overinterpreting the results of the mutagenesis study.

On the basis of the evidence that Glu 197β is a catalytic residue, a second residue in site II, Tyr 109β, must also be important for catalysis. In the structure of the wild-type SCS, the side chain of Glu 197β accepts a hydrogen bond from the hydroxyl group of Tyr 109β. Like the glutamate residue, this residue is conserved among all known sequences of the β-subunit of succinyl-CoA synthetase (*34*), the sole exception being the hypothetical β-subunit of cyanobacterium *Synechocystis sp.* strain PCC6803 where the equivalent residue is phenylalanine (*35*). The tyrosine residue of SCS can be compared to Thr 189 in the structure of DD-ligase (*8*). In the complex of DD-ligase with ADP, Mg^{2+} ions and the phosphorylated phosphinate analogue, Thr 189 accepts a hydrogen bond from Arg 255, the residue equivalent to Glu 197β of SCS. Thr 189 also donates a hydrogen bond to Asp 257, likely aiding in orienting the side chain carboxylate group to coordinate one of the Mg^{2+} ions. In contrast to DD-ligase, SCS has a backbone atom, the carbonyl oxygen atom of the Asn-Pro *cis*-peptide bond, to coordinate the equivalent Mg^{2+} ion, so another residue would not be needed to orient this oxygen atom. The role of Tyr 109β in SCS would be to position Glu 197β for catalysis in site II.

Looking more broadly to other enzymes possessing the ATP-grasp fold, we can hypothesize that the residues equivalent to Glu 197β and Tyr 109β are important in catalysis by these phosphorylating enzymes. Like DD-ligase, glutathione synthetase phosphorylates a carboxylate group. The guanidinium moiety of Arg 210 of glutathione synthetase interacts with the oxygen atom of the cysteine−glycine peptide bond of glutathione as well as with the sulfate ion in the complex with Mg^{2+}-ADP, glutathione, and a sulfate ion (*36*). The sulfate ion is similar to phosphate, so this complex is thought to represent a pseudo enzyme−substrate complex. Arg 210 is not in the position equivalent to Arg

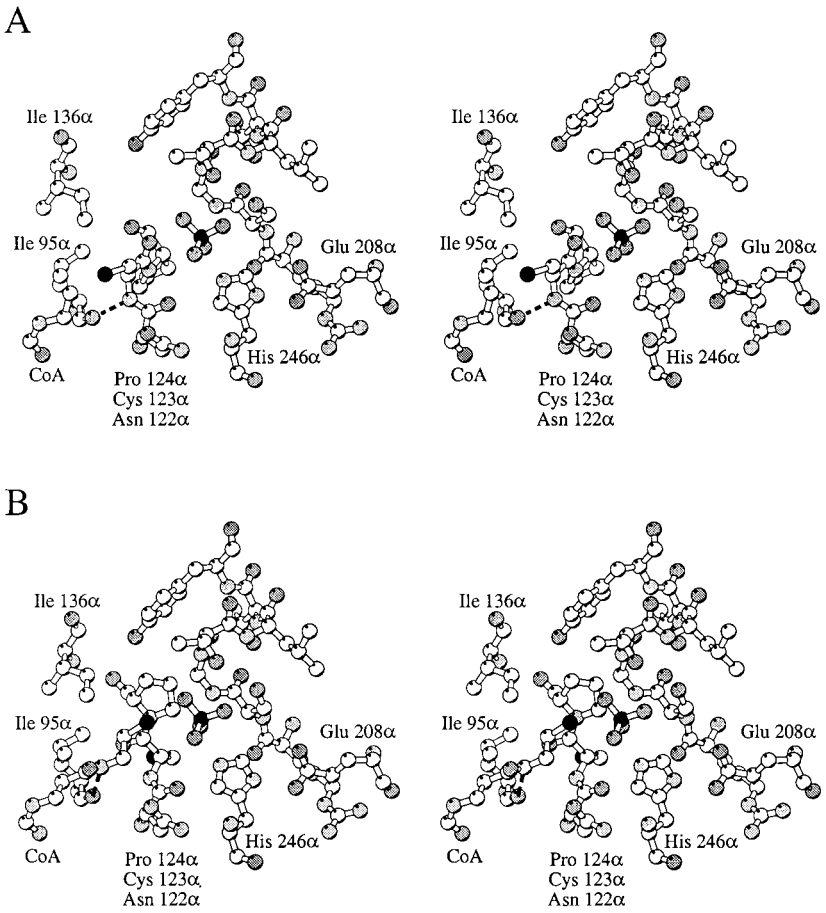

FIGURE 6: Site I of (A) the E197βA mutant protein and (B) wild-type SCS. Both structures are shown in the same orientation, as ball-and-stick models in stereo. The atom shading is according to type, the darkest being the heaviest atom, phosphorus, and the lightest, carbon. The hydrogen bond between the carbonyl oxygen atom of Ile 95α and the nitrogen atom of Cys 123α in panel A or atom PN4 of the CoA molecule in panel B is represented by a dashed line.

255 of DD-ligase, where instead there is a glycine residue, Gly 271, in glutathione synthetase, but it is in the position equivalent to Thr 189 of DD-ligase and Tyr 109β of SCS. Like glutathione synthetase, synapsin I has an arginine residue, Arg 315, in the second position, and in the structure, this residue that is conserved in synapsins Ia, IIa, and IIIa (*37*) reaches across a conserved alanine residue, Ala 371, toward the nucleotide-binding site. Ala 371 is in the equivalent position to Gly 271 of glutathione synthetase. A substrate of synapsin I is not known. However, since synapsin I has this conserved arginine residue, we predict that it phosphorylates a carboxylate group of its substrate.

The inability of succinyl-CoA and $^{32}P_i$ to phosphorylate the E197βA mutant protein was a surprising result. This mutation at site II would be expected to impair phosphorylation by nucleotide, but was not expected to affect phosphorylation by succinyl-CoA and $^{32}P_i$ at site I more than 30 Å away. This mutation impaired the full reaction, reducing the activity to such an extent that the mutant protein was inactive (under normal conditions) and no kinetic parameters could be determined. The E197βA mutant protein did crystallize, suggesting that it was properly folded and that it bound CoA. This crystal form of *E. coli* SCS requires stoichiometric amount of CoA (*25*) because the CoA molecules bound to each α-subunit of the heterotetramer form part of the crystal-packing interface (*6*, *38*). The crystallographic analysis proved that the E197βA mutant protein bound CoA.

The crystal structure determination of the E197βA mutant protein showed no significant conformational changes in the vicinity of the mutation, other than the reduced electron density expected for an alanine residue. Although Tyr 109β no longer has the side chain of residue 197β with which to interact, it adopts similar torsion angles as in the wild-type enzyme. This is because of van der Waals interactions with other residues of the β-subunit: Met 124β, Ile 133β, and Asn 199β. The significant difference between the structure of wild-type SCS and that of the E197βA mutant protein was located at site I, 30 Å away from the mutation. Two residues of the α-subunit, Cys 123α−Pro 124α, adopt a conformation that is significantly different from that in the native structure. Figure 6 shows how the side chain of Cys 123α is exposed, occupying the similar position to that of the free thiol of the CoA molecule in the structure of the wild-type enzyme. Furthermore, the side chain of the proline residue is buried in the position normally occupied by the cysteine side chain. We interpret the absence of electron density for the six atoms of the CoA molecule as indicating that this moiety is disordered. In the structure of wild-type SCS, atom PN4 of the CoA molecule donates a hydrogen bond to the carbonyl oxygen atom of Ile 95α (*6*). In the structure of the E197βA mutant protein, this carbonyl oxygen atom accepts a hydrogen bond from the amide nitrogen atom of Cys 123α in its "new" conformation—the side chain of Cys 123α would hinder any hydrogen-bonding interaction between the protein and PN4 of the CoA molecule. The

E197βA mutant protein still binds the nucleotide moiety of CoA, but since Cys 123α is located between the nucleotide moiety of CoA and the active-site histidine residue, this cysteine residue effectively excludes the thiol end of CoA from the vicinity of the active-site histidine residue. Thus, the succinyl moiety of succinyl-CoA would also be disordered, excluded from the binding site of the phosphate ion and the active-site histidine residue. Therefore, our conclusion is that succinyl-CoA and P_i cannot phosphorylate this mutant protein because Cys 123α is in a conformation whereby it effectively blocks the binding site for the succinyl moiety, preventing partial reaction 1, the formation of succinyl-phosphate, from occurring.

The conformational change at Cys 123α−Pro 124α results in the loss of one hydrogen bond between the protein and the CoA molecule and would therefore reduce the free energy change on binding CoA. However, this hydrogen bond provides a minor contribution to the binding, given the number of other interactions that the CoA molecule makes with the α-subunit. Seven other direct hydrogen bonds between the substrate and the protein are maintained, and the buried surface area is still 87% of that buried in the complex of CoA with the wild-type enzyme (*39*). (For this calculation, it was assumed that the surface area of CoA would be the same in either complex.) The interpretation from the crystal structure is that the dissociation constant for CoA with the E197βA mutant protein would be similar to that with the wild-type enzyme.

The structure of the E197βA mutant protein suggests that when the α-subunit of SCS folds, the side chain of Cys 123α is exposed, and the side chain of Pro 124α is directed to the interior of the protein. We hypothesize that normally phosphorylation of the active-site histidine residue by ATP or GTP induces the conformational change at Cys 123α−Pro 124α. This is the simplest explanation of how a mutant protein that cannot be phosphorylated by ATP or GTP has a different conformation for these residues located so far from the mutation.

This alternate conformation of Cys 123α−Pro 124α was first observed in the structure of wild-type SCS in complex with ADP and Mg^{2+} ions, but its relevance was not known (*4*). To form this complex, the crystals had been transferred to solutions containing lowered concentrations of sulfate and phosphate ions and increased concentrations of ADP and Mg^{2+} ions (in the absence of a reducing agent). In this structure, Cys 123α appeared to be linked by a disulfide bond with the free thiol group of the CoA molecule. We conclude that during the soak with nucleotide, the conformational change at Cys 123α−Pro 124α occurred and the nonphysiological disulfide bond served to trap the side chain of Cys 123α on the surface of the protein. Although we do not think that the formation of the disulfide bond between Cys 123α and the CoA molecule is part of the catalytic mechanism of SCS, we do hypothesize that the conformational change of Cys 123α−Pro 124α has a functional role. The fact that the residues in this region of the α-subunit, Gly−Pro−Asn−Cys−Pro−Gly, are among the most conserved in succinyl-CoA synthetases (*34*) is consistent with this hypothesis. Exactly how phosphorylation of the active-site histidine residue by the nucleotide at site II induces a conformational change 30 Å away at site I is yet to be discovered.

ACKNOWLEDGMENT

We would like to acknowledge the work of Edward Brownie in producing and purifying wild-type SCS and the mutant proteins. We thank Ken Ng and Ernst Bergmann for collecting the data set for the E197βA mutant protein at SSRL.

REFERENCES

1. Bridger, W. A. (1974) in *The Enzymes* (Boyer, P. D., Ed.) Academic Press, New York, pp 581−606.
2. Nishimura, J. S. (1986) in *Advances in Enzymology* (Meister, A., Ed.) pp 141−172, Wiley, New York.
3. Wolodko, W. T., Fraser, M. E., James, M. N. G., and Bridger, W. A. (1994) *J. Biol. Chem. 269*, 10883−10890.
4. Joyce, M. A., Fraser, M. E., James, M. N. G., Bridger, W. A., and Wolodko, W. T. (2000) *Biochemistry 39*, 17−25.
5. Fraser, M. E., James, M. N. G., Bridger, W. A., and Wolodko, W. T. (2000) *J. Mol. Biol. 299*, 1325−1339.
6. Fraser, M. E., James, M. N. G., Bridger, W. A., and Wolodko, W. T. (1999) *J. Mol. Biol. 285*, 1633−1653.
7. Joyce, M. A., Fraser, M. E., Brownie, E. R., James, M. N. G., Bridger, W. A., and Wolodko, W. T. (1999) *Biochemistry 38*, 7273−7283.
8. Fan, C., Moews, P. C., Walsh, C. T., and Knox, J. R. (1994) *Science 266*, 439−443.
9. Murzin, A. G. (1996) *Curr. Opin. Struct. Biol. 6*, 386-394.
10. Yamaguchi, H., Kato, H., Hata, Y., Nishioka, T., Kimura, A., Oda, J., and Katsube, Y. (1993) *J. Mol. Biol. 229*, 1083−1100.
11. Waldrop, G. L., Rayment, I., and Holden, H. M. (1994) *Biochemistry 33*, 10249−10256.
12. Herzberg, O., Chen, C. C. H., Kapadia, G., McGuire, M., Carroll, L., Noh, S. J., and Dunaway-Mariano, D. (1996) *Proc. Natl. Acad. Sci. U.S.A. 93*, 2652−2657.
13. Subramanya, H. S., Doherty, A. J., Ashford, S. R., and Wigley, D. B. (1996) *Cell 85*, 607−615.
14. Hakansson, K., Doherty, A. J., Shuman, S., and Wigley, D. B. (1997) *Cell 89*, 545−553.
15. Thoden, J. B., Holden, H. M., Wesenberg, G., Raushel, F. M., and Rayment, I. (1997) *Biochemistry 36*, 6305−6316.
16. Esser, L., Wang, C., Hosaka, M., Smagula, C. S., Sudhof, T. C., and Deisenhofer, J. (1998) *EMBO J. 17*, 977−984.
17. Wang, W., Kappock, T. J., Stubbe, J., and Ealick, S. E. (1998) *Biochemistry 37*, 15647−15662.
18. Thoden, J. B., Kappock, T. J., Stubbe, J., and Holden, H. M. (1999) *Biochemistry 38*, 15480−15492.
19. Ho, S., Hunt, H., Horton, R., Pullen, J., and Pease, L. (1989) *Gene 77*, 51−59.
20. Buck, D., and Guest, J. R. (1989) *Biochem. J. 260*, 737−747.
21. Rhodes, D. B., Laimins, L., and Epstein, W. (1978) *J.Bacteriol. 135*, 445−452.
22. Wolodko, W. T., Kay, C. M., and Bridger, W. A. (1986) *Biochemistry 25*, 5420−5425.
23. Krebs, A., and Bridger, W. A. (1974) *Can. J. Biochem. 52*, 594−598.
24. Stanislawski, J. (1991) *Enzyme Kinetics*, Trinity Software, Campton, NH.
25. Wolodko, W. T., James, M. N. G., and Bridger, W. A. (1984) *J. Biol. Chem. 259*, 5316−5320.
26. Szebenyi, D. M. E., Arvai, A., Ealick, S., LaIuppa, J. M., and Nielsen, C. (1997) *J. Synchrotron Radiat. 4*, 128−135.
27. Otwinowski, Z., and Minor, W. (1997) in *Methods in Enzymology* (Carter, C. W., Jr., and Sweet, R. M., Eds.) pp 307−326, Academic Press, New York.
28. Brünger, A. T., Adams, P. D., Clore, G. M., Delano, W. L., Gros, P., Grosse-Kunstleve, R. W., Jiang, J.-S., Kuszewski, J., Jilges, N., Pannu, N. S., Read, R. J., Rice, L. M., Simonson, T., and Warren, G. L. (1998) *Acta Crystallogr., Sect. D 54*, 905−921.
29. Jones, T. A. (1985) in *Methods in Enzymology* (Wyckoff, H. W., Hirs, C. H. W., and Timasheff, S. N., Ed.) pp 157−171, Academic Press, New York.

30. Laskowski, R. A., MacArthur, M. W., Moss, D. S., and Thornton, J. M. (1993) *J. Appl. Crystallogr. 26*, 283−291.
31. Hooft, R. W. W., Vriend, G., Sander, C., and Abola, E. E. (1996) *Nature 381*, 272.
32. Collaborative Computational Project, No. 4 (1994) *Acta Crystallogr., Sect. D 50*, 760−763.
33. Berman, H. M., Westbrook, J., Feng, Z., Gilliland, G., Bhat, T. N., Weissig, H., Shindyalov, I. N., and Bourne, P. E. (2000) *Nucleic Acids Res. 28*, 235−242.
34. Altschul, S. F., Madden, T. L., Schaffer, A. A., Zhang, J., Zhang, Z., Miller, W., and Lipman, D. J. (1997) *Nucleic Acids Res. 25*, 3389−3402.
35. Kaneko, T., Sato, S., Kotani, H., Tanaka, A., Asamizu, E., Nakamura, Y., Miyajima, N., Hirosawa, M., Sugiura, M., Sasamoto, S., Kimura, T., Hosouchi, T., Matsuno, A., Muraki, A., Nakazaki, N., Naruo, K., Okumura, S., Shimpo, S., Takeuchi, C., Wada, T., Watanabe, A., Yamada, M., Yasuda, M., and Tabata, S. (1996) *DNA Res. 3*, 109−136.
36. Hara, T., Kato, H., Katsube, Y., and Oda, J. (1996) *Biochemistry 35*, 11967−11974.
37. Hosaka, M., and Sudhof, T. C. (1998) *J. Biol. Chem. 273*, 13371−13374.
38. Bailey, D. L., Fraser, M. E., Bridger, W. A., James, M. N. G., and Wolodko, W. T. (1999) *J. Mol. Biol. 285*, 1655−1666.
39. Connolly, M. L. (1983) *Science 221*, 709−713.
40. Kraulis, P. J. (1991) *J. Appl. Crystallogr. 24*, 946−950.

BI011518Y